EUROPEAN ORGANISATION FOR NUCLEAR RESEARCH

CERN-PPE/95-153
26 October 1995

J/ψ and ψ' production in hadronic Z^0 decays

The OPAL Collaboration

Abstract

The production of J/ψ mesons in Z^0 decays is studied using 3.6 million hadronic events recorded by the OPAL detector at LEP. The inclusive Z^0 to J/ψ and b-quark to J/ψ branching ratios are measured from the total yield of J/ψ mesons, identified from their decays into lepton pairs. The J/ψ momentum distribution is used to study the fragmentation of b-quarks. The production rate of ψ' mesons, identified from their decays into a J/ψ and a $\pi^+\pi^-$ pair, is measured as well. The following results are obtained:

$$Br(Z^0 \to J/\psi\ X) = (3.9 \pm 0.2 \pm 0.3) \cdot 10^{-3} \qquad \text{and}$$

$$Br(Z^0 \to \psi'\ X) = (1.6 \pm 0.3 \pm 0.2) \cdot 10^{-3},$$

where the first error is statistical and the second systematic. Finally the J/ψ sample is used to reconstruct exclusive b-hadron decays and calculate the corresponding b-hadron branching ratios and masses.

(To be submitted to Zeitschrift für Physik C)

The OPAL Collaboration

G. Alexander[23], J. Allison[16], N. Altekamp[5], K. Ametewee[25], K.J. Anderson[9], S. Anderson[12], S. Arcelli[2], S. Asai[24], D. Axen[29], G. Azuelos[18,a], A.H. Ball[17], E. Barberio[26], R.J. Barlow[16], R. Bartoldus[3], J.R. Batley[5], G. Beaudoin[18], J. Bechtluft[14], G.A. Beck[13], C. Beeston[16], T. Behnke[8], A.N. Bell[1], K.W. Bell[20], G. Bella[23], S. Bentvelsen[8], P. Berlich[10], S. Bethke[14], O. Biebel[14], I.J. Bloodworth[1], J.E. Bloomer[1], P. Bock[11], H.M. Bosch[11], M. Boutemeur[18], B.T. Bouwens[12], S. Braibant[12], P. Bright-Thomas[25], R.M. Brown[20], H.J. Burckhart[8], C. Burgard[27], R. Bürgin[10], P. Capiluppi[2], R.K. Carnegie[6], A.A. Carter[13], J.R. Carter[5], C.Y. Chang[17], C. Charlesworth[6], D.G. Charlton[1,b], D. Chrisman[4], S.L. Chu[4], P.E.L. Clarke[15], S.G. Clowes[16], I. Cohen[23], J.E. Conboy[15], O.C. Cooke[16], M. Cuffiani[2], S. Dado[22], C. Dallapiccola[17], G.M. Dallavalle[2], C. Darling[31], S. De Jong[12], L.A. del Pozo[8], M.S. Dixit[7], E. do Couto e Silva[12], E. Duchovni[26], G. Duckeck[8], I.P. Duerdoth[16], U.C. Dunwoody[8], J.E.G. Edwards[16], P.G. Estabrooks[6], H.G. Evans[9], F. Fabbri[2], B. Fabbro[21], P. Fath[11], F. Fiedler[12], M. Fierro[2], M. Fincke-Keeler[28], H.M. Fischer[3], R. Folman[26], D.G. Fong[17], M. Foucher[17], H. Fukui[24], A. Fürtjes[8], P. Gagnon[7], A. Gaidot[21], J.W. Gary[4], J. Gascon[18], S.M. Gascon-Shotkin[17], N.I. Geddes[20], C. Geich-Gimbel[3], S.W. Gensler[9], F.X. Gentit[21], T. Geralis[20], G. Giacomelli[2], P. Giacomelli[4], R. Giacomelli[2], V. Gibson[5], W.R. Gibson[13], D.M. Gingrich[30,a], J. Goldberg[22], M.J. Goodrick[5], W. Gorn[4], C. Grandi[2], E. Gross[26], C. Hajdu[32], G.G. Hanson[12], M. Hansroul[8], M. Hapke[13], C.K. Hargrove[7], P.A. Hart[9], C. Hartmann[3], M. Hauschild[8], C.M. Hawkes[8], R. Hawkings[8], R.J. Hemingway[6], G. Herten[10], R.D. Heuer[8], M.D. Hildreth[8], J.C. Hill[5], S.J. Hillier[8], T. Hilse[10], P.R. Hobson[25], D. Hochman[26], R.J. Homer[1], A.K. Honma[28,a], D. Horváth[32,c], R. Howard[29], R.E. Hughes-Jones[16], D.E. Hutchcroft[5], P. Igo-Kemenes[11], D.C. Imrie[25], A. Jawahery[17], P.W. Jeffreys[20], H. Jeremie[18], M. Jimack[1], A. Joly[18], M. Jones[6], R.W.L. Jones[8], U. Jost[11], P. Jovanovic[1], D. Karlen[6], T. Kawamoto[24], R.K. Keeler[28], R.G. Kellogg[17], B.W. Kennedy[20], B.J. King[8], J. King[13], J. Kirk[29], S. Kluth[5], T. Kobayashi[24], M. Kobel[10], D.S. Koetke[6], T.P. Kokott[3], S. Komamiya[24], R. Kowalewski[8], T. Kress[11], P. Krieger[6], J. von Krogh[11], P. Kyberd[13], G.D. Lafferty[16], H. Lafoux[21], R. Lahmann[17], W.P. Lai[19], D. Lanske[14], J. Lauber[15], J.G. Layter[4], A.M. Lee[31], E. Lefebvre[18], D. Lellouch[26], J. Letts[2], L. Levinson[26], C. Lewis[15], S.L. Lloyd[13], F.K. Loebinger[16], G.D. Long[17], B. Lorazo[18], M.J. Losty[7], J. Ludwig[10], A. Luig[10], A. Malik[21], M. Mannelli[8], S. Marcellini[2], C. Markus[3], A.J. Martin[13], J.P. Martin[18], G. Martinez[17], T. Mashimo[24], W. Matthews[25], P. Mättig[3], W.J. McDonald[30], J. McKenna[29], E.A. Mckigney[15], T.J. McMahon[1], A.I. McNab[13], F. Meijers[8], S. Menke[3], F.S. Merritt[9], H. Mes[7], J. Meyer[27], A. Michelini[8], G. Mikenberg[26], D.J. Miller[15], R. Mir[26], W. Mohr[10], A. Montanari[2], T. Mori[24], M. Morii[24], U. Müller[3], B. Nellen[3], B. Nijjhar[16], R. Nisius[8], S.W. O'Neale[1], F.G. Oakham[7], F. Odorici[2], H.O. Ogren[12], N.J. Oldershaw[16], T. Omori[24], C.J. Oram[28,a], M.J. Oreglia[9], S. Orito[24], M. Palazzo[2], J. Pálinkás[33], F.M. Palmonari[2], J.P. Pansart[21], G. Pásztor[33], J.R. Pater[16], G.N. Patrick[20], M.J. Pearce[1], P.D. Phillips[16], J.E. Pilcher[9], J. Pinfold[30], D.E. Plane[8], P. Poffenberger[28], B. Poli[2], A. Posthaus[3], T.W. Pritchard[13], H. Przysiezniak[30], D.L. Rees[1], D. Rigby[1], M.G. Rison[5], S.A. Robins[13], N. Rodning[30], J.M. Roney[28], E. Ros[8], A.M. Rossi[2], M. Rosvick[28], P. Routenburg[30], Y. Rozen[8], K. Runge[10], O. Runolfsson[8], D.R. Rust[12], R. Rylko[25], E.K.G. Sarkisyan[23], M. Sasaki[24], C. Sbarra[2], A.D. Schaile[8], O. Schaile[10], F. Scharf[3], P. Scharff-Hansen[8], P. Schenk[4], B. Schmitt[3], M. Schröder[8], H.C. Schultz-Coulon[10], M. Schulz[8], P. Schütz[3], J. Schwiening[3], W.G. Scott[20], T.G. Shears[16], B.C. Shen[4], C.H. Shepherd-Themistocleous[27], P. Sherwood[15], G.P. Siroli[2], A. Sittler[27], A. Skillman[15], A. Skuja[17], A.M. Smith[8], T.J. Smith[28], G.A. Snow[17], R. Sobie[28], S. Söldner-Rembold[10], R.W. Springer[30], M. Sproston[20], A. Stahl[3], M. Starks[12], C. Stegmann[10], K. Stephens[16], J. Steuerer[28], B. Stockhausen[3], D. Strom[19], F. Strumia[8], P. Szymanski[20], R. Tafirout[18], H. Takeda[24], P. Taras[18], S. Tarem[22], M. Tecchio[8], N. Tesch[3], M.A. Thomson[8], E. von Törne[3], S. Towers[6], M. Tscheulin[10], T. Tsukamoto[24], E. Tsur[23], A.S. Turcot[9], M.F. Turner-Watson[8], P. Utzat[11], R. Van Kooten[12], G. Vasseur[21], P. Vikas[18], M. Vincter[28], E.H. Vokurka[16], F. Wäckerle[10], A. Wagner[27], D.L. Wagner[9],

C.P. Ward[5], D.R. Ward[5], J.J. Ward[15], P.M. Watkins[1], A.T. Watson[1], N.K. Watson[7], P. Weber[6], P.S. Wells[8], N. Wermes[3], B. Wilkens[10], G.W. Wilson[27], J.A. Wilson[1], T. Wlodek[26], G. Wolf[26], S. Wotton[11], T.R. Wyatt[16], S. Xella[2], S. Yamashita[24], G. Yekutieli[26], V. Zacek[18],

[1]School of Physics and Space Research, University of Birmingham, Birmingham B15 2TT, UK
[2]Dipartimento di Fisica dell' Università di Bologna and INFN, I-40126 Bologna, Italy
[3]Physikalisches Institut, Universität Bonn, D-53115 Bonn, Germany
[4]Department of Physics, University of California, Riverside CA 92521, USA
[5]Cavendish Laboratory, Cambridge CB3 0HE, UK
[6] Ottawa-Carleton Institute for Physics, Department of Physics, Carleton University, Ottawa, Ontario K1S 5B6, Canada
[7]Centre for Research in Particle Physics, Carleton University, Ottawa, Ontario K1S 5B6, Canada
[8]CERN, European Organisation for Particle Physics, CH-1211 Geneva 23, Switzerland
[9]Enrico Fermi Institute and Department of Physics, University of Chicago, Chicago IL 60637, USA
[10]Fakultät für Physik, Albert Ludwigs Universität, D-79104 Freiburg, Germany
[11]Physikalisches Institut, Universität Heidelberg, D-69120 Heidelberg, Germany
[12]Indiana University, Department of Physics, Swain Hall West 117, Bloomington IN 47405, USA
[13]Queen Mary and Westfield College, University of London, London E1 4NS, UK
[14]Technische Hochschule Aachen, III Physikalisches Institut, Sommerfeldstrasse 26-28, D-52056 Aachen, Germany
[15]University College London, London WC1E 6BT, UK
[16]Department of Physics, Schuster Laboratory, The University, Manchester M13 9PL, UK
[17]Department of Physics, University of Maryland, College Park, MD 20742, USA
[18]Laboratoire de Physique Nucléaire, Université de Montréal, Montréal, Quebec H3C 3J7, Canada
[19]University of Oregon, Department of Physics, Eugene OR 97403, USA
[20]Rutherford Appleton Laboratory, Chilton, Didcot, Oxfordshire OX11 0QX, UK
[21]CEA, DAPNIA/SPP, CE-Saclay, F-91191 Gif-sur-Yvette, France
[22]Department of Physics, Technion-Israel Institute of Technology, Haifa 32000, Israel
[23]Department of Physics and Astronomy, Tel Aviv University, Tel Aviv 69978, Israel
[24]International Centre for Elementary Particle Physics and Department of Physics, University of Tokyo, Tokyo 113, and Kobe University, Kobe 657, Japan
[25]Brunel University, Uxbridge, Middlesex UB8 3PH, UK
[26]Particle Physics Department, Weizmann Institute of Science, Rehovot 76100, Israel
[27]Universität Hamburg/DESY, II Institut für Experimental Physik, Notkestrasse 85, D-22607 Hamburg, Germany
[28]University of Victoria, Department of Physics, P O Box 3055, Victoria BC V8W 3P6, Canada
[29]University of British Columbia, Department of Physics, Vancouver BC V6T 1Z1, Canada
[30]University of Alberta, Department of Physics, Edmonton AB T6G 2J1, Canada
[31]Duke University, Dept of Physics, Durham, NC 27708-0305, USA
[32]Research Institute for Particle and Nuclear Physics, H-1525 Budapest, P O Box 49, Hungary
[33]Institute of Nuclear Research, H-4001 Debrecen, P O Box 51, Hungary

[a]Also at TRIUMF, Vancouver, Canada V6T 2A3
[b] Royal Society University Research Fellow
[c] Institute of Nuclear Research, Debrecen, Hungary

1 Introduction

J/ψ mesons are produced in Z^0 decays predominantly via b-hadron decays and can be identified from their decays into lepton pairs. A small number are expected to be produced in fragmentation processes. The production of 'colour-singlet' J/ψ in fragmentation processes has been calculated using perturbative QCD and is found to be negligible (a summary of the various 'colour-singlet' models is given in [1]). These models fail however to explain the unexpectedly large production of quarkonia at the Tevatron. It has been proposed to consider 'colour-octet' models to explain this discrepancy between theory and experimental data (see [2] and references therein). In these models, the J/ψ is first produced in a 'colour-octet' state and then evolves into a 'colour-singlet' state by emission of soft gluons. These 'colour-octet' models predict a sizable production of J/ψ in Z^0 decays as well [3].

In all of these processes (b-quark decays and fragmentation), the J/ψ is produced either directly or via the decay of other charmonium states like χ_{c1} and ψ' mesons[1]. According to theoretical calculations [4], charmonium states are produced in b-hadron decays in the following proportions:

$$\eta_c : J/\psi \ : \chi_{c1} : \psi' \ = 0.57 : 1 : 0.27 : 0.31.$$

The inclusive production of J/ψ in Z^0 decays has already been measured by OPAL [5] and by the other LEP experiments [6, 7, 8]. ψ' and χ_{c1} mesons can be identified using their decays into a J/ψ and a $\pi^+\pi^-$ pair or a photon, respectively. Evidence for the production of ψ' and χ_{c1} mesons has been found in this way, both in $\Upsilon(4S)$ decays [9] and in Z^0 decays [7, 8]. In this paper, inclusive measurements of the J/ψ and ψ' production ratios are presented, using a considerably enlarged multihadronic sample compared to that in the previous OPAL J/ψ analysis [5]. The increased statistics allow additional studies of b-quark fragmentation.

J/ψ decays represent a clear signature for individual b-hadrons [10]. If the b-hadron can be fully reconstructed, these decays provide clean mass and lifetime measurements. The low-multiplicity modes $B^0 \to J/\psi\, K^0_S$, $B^0 \to J/\psi\, K^{*0}$, $B^+ \to J/\psi\, K^+$, have been observed with significant statistics in $p\bar{p}$ collisions [11] and in $\Upsilon(4S)$ decays [12], and with marginal statistics in Z^0 decays [6, 8]. The observation of a few decays in the modes $B_s \to J/\psi\,\phi$ and $B_s \to \psi'\phi$ has been decisive for the discovery of the B_s and the measurement of its mass [13, 14, 15, 16]. The observation of the decay $\Lambda_b \to J/\psi\,\Lambda$ would be of similar importance for Λ_b baryons. A first observation of this decay in $p\bar{p}$ collisions [17] is however not confirmed by more recent measurements [18], and no signal has been reported in Z^0 decays either. Similarly, a search for the yet unobserved B_c meson can be performed using the decay mode $B_c \to J/\psi\,\pi^+$. In this paper, a search for low multiplicity b-hadron decays is presented, and the reconstructed decays are used to calculate b-hadron decay rates and masses. The statistics are however insufficient to study other b-hadron properties.

The outline of this paper is as follows: the OPAL detector is briefly described in section 2, the inclusive J/ψ analysis, including event selection requirements, the inclusive branching ratio and a b-quark fragmentation analysis, is presented in section 3, a search for ψ' mesons decaying into a J/ψ and a $\pi^+\pi^-$ pair is presented in section 4, and finally a search for exclusive b-hadron decays into J/ψ is presented in section 5.

2 The OPAL detector

The OPAL detector is a multi–purpose apparatus installed at the electron–positron collider LEP. A detailed description of its layout and performance can be found in [19]. The detector components that are relevant to this analysis are briefly mentioned below. Tracking of charged particles is performed using the central detector which is contained in a magnetic field of 0.435 T. The central tracking system consists of a two layer silicon microstrip vertex detector, a high precision drift chamber, a large volume

[1] ψ' mesons are also referred to as $\psi(2S)$ or $\psi(3685)$.

jet chamber and a set of z chambers measuring the track coordinates along the beam direction[2]. The silicon microvertex detector [20], operational from 1991 onwards, allows a reconstruction of secondary vertices in each event with high precision in the r–ϕ plane. Particle identification is provided by the measurement of the specific ionisation loss, $\mathrm{d}E/\mathrm{d}x$, in the jet chamber [21]. The $\mathrm{d}E/\mathrm{d}x$ resolution obtained in multihadronic events for minimum ionising particles with the maximum of 159 ionisation samples is 3.5%. The momentum resolution of the central detector in the plane perpendicular to the beam axis is $(\sigma_{p_t}/p_t)^2 = (0.02)^2 + (0.0015 \cdot p_t)^2$, where p_t is given in [GeV/c]. The central detector is surrounded by a lead glass electromagnetic calorimeter, which is equipped with a presampler. Beyond this are the hadron calorimeter and the muon chambers.

3 Inclusive J/ψ production

3.1 Event, lepton and J/ψ selection

The initial multihadron sample was defined using standard OPAL criteria [22]. Tracks were required to satisfy minimum quality cuts as in [23]. Only events with at least 7 tracks passing these quality cuts were considered. After all cuts, a total of 3.6 million hadronic events were selected. The selection efficiency for this hadronic sample is $(98.1 \pm 0.5)\%$, and the background is less than 0.1%. The flavour-bias for b-quark events introduced by this selection was determined to be less than 0.1% using simulated events. A sample of 10 000 Monte Carlo (MC) events containing the decay chain $\mathrm{Z^0 \to b\bar{b} \to J/\psi \to \ell^+\ell^-}$, generated using JETSET 7.4 [24] with parameter settings as in [25] and with full detector simulation [26] has been used to calculate selection efficiencies. These events were generated using the Peterson fragmentation function for b-quarks [27]. A sample of about 2 million MC events containing hadronic $\mathrm{Z^0}$ decays has been used to deduce corrections to the efficiency based on a comparison between various data and MC distributions. Finally, a sample of 2000 MC events simulating the fragmentation process described in [3] has been used to determine selection efficiencies and momentum spectra. In this simulation, JETSET 7.4 was used for parton hadronisation and particle decay processes.

Lepton candidates were required to satisfy the following kinematic and geometrical cuts:

- $p > 2$ GeV/c, where p is the track momentum.
- $|\cos\theta| < 0.9$, where θ is the polar angle with respect to the electron beam direction.

In order to ensure sufficient track quality for the calculation of the invariant mass, an accurate polar angle measurement (z chamber match, for barrel tracks, or constraint to the point where the track leaves the jet chamber, in the case of forward tracks) was required for all lepton tracks. A second requirement that at least 10 hits were used for the calculation of the ionisation energy loss eliminates tracks too close to other tracks or to the anode and cathode planes of the central detector. Lepton identification with the OPAL detector is described in detail in [23]. The selection requirements used in the present analysis are briefly described below.

The following electron identification requirements were applied:

- $(\mathrm{d}E/\mathrm{d}x)_{\mathrm{norm}} > -2.0$, where $(\mathrm{d}E/\mathrm{d}x)_{\mathrm{norm}}$ is a normalised $\mathrm{d}E/\mathrm{d}x$ value defined as:

$$(\mathrm{d}E/\mathrm{d}x)_{\mathrm{norm}} = [\mathrm{d}E/\mathrm{d}x - (\mathrm{d}E/\mathrm{d}x)_0]/\sigma(\mathrm{d}E/\mathrm{d}x),$$

  $\mathrm{d}E/\mathrm{d}x$ being the measured track ionisation energy loss per unit length, $(\mathrm{d}E/\mathrm{d}x)_0$ the average $\mathrm{d}E/\mathrm{d}x$ for electrons at the measured momentum, and $\sigma(\mathrm{d}E/\mathrm{d}x)$ the resolution on $\mathrm{d}E/\mathrm{d}x$ for the candidate track.

- $E/p > 0.7$, where E is the electromagnetic energy associated with the track, as defined in [28].

[2]The OPAL right-handed coordinate system is defined with positive z being along the electron beam direction, and θ and ϕ being the polar and azimuthal angles, respectively.

- Electrons identified as originating in photon conversions by the algorithm described in [23] were rejected.

The following muon identification requirements were applied:

- $\chi_{\rm pos} < 3$, where $\chi_{\rm pos}$ is a positional matching parameter, defined as the distance between the extrapolated candidate track and a muon segment reconstructed in the external muon chambers, normalised by the expected error on that distance at the position of the muon chambers.
- Only the best segment match for each track and the best track for each segment is considered.

J/ψ candidates were selected by demanding two electron or two muon tracks of opposite charge, with an opening angle smaller than 60° and with invariant mass in the range 2.9–3.3 GeV/c^2. The total number of J/ψ candidates in the data sample is $N_{\rm cand}$=741.

3.2 Background and efficiency

The background of the J/ψ sample has been calculated directly from the data, using 'wrong lepton combinations'. These combinations are opposite charge track pairs formed by an electron and a muon, but passing otherwise the same selection criteria as J/ψ candidates. These events provide an exact description of the background only in the limit of equal efficiency and background for the electron and muon selection. In case of differences between electrons and muons, this method underestimates the background and a scaling factor is needed. This scaling factor has been obtained from the ratio between the number of $e^+e^- + \mu^+\mu^-$ pairs and the number of $e^\pm\mu^\mp$ pairs in the invariant mass interval 2.0–4.0 GeV/c^2, after excluding the region 2.8–3.3 GeV/c^2. The correction to the scaling factor introduced by J/ψ and ψ' lepton pairs outside the signal region is -6.4% and -1.3%, respectively. After applying this correction, the result is $1.01 \pm 0.03 \pm 0.03$, where the first error is statistical and the second error results from the correction. The background is then (see Fig. 1) $N_{\rm bkg} = 230 \pm 18$ events, where the error includes both statistical and scaling factor uncertainties. The background subtracted number of J/ψ candidates is therefore

$$N_{\rm J/\psi} = N_{\rm cand} - N_{\rm bkg} = 511 \pm 27 \pm 18,$$

where the first error is statistical and the second results from the background subtraction. An alternative method to determine the background using a fitting function has been used as a cross-check. The fitting function consists of an exponential to describe the background and two Gaussians with radiative tails, to describe the J/ψ and ψ' signals. The radiative tails account for both bremsstrahlung radiation in the detector and final state radiation in J/ψ and ψ' decays (see below). The shape of the exponential used to describe the background was adjusted to the $e^\pm\mu^\mp$ invariant mass distribution and the function used to describe the signal was obtained from the MC. The normalisation of the J/ψ and ψ' signals and that of the background were allowed to vary. The result of this fit (see Fig. 2) is a background of $N_{\rm bkg} = 237 \pm 16$, compatible with the previous value. The error on this background number does not include any uncertainty related to the shape of the signal. Taking into account the reduced leptonic branching ratio and the production rate from b-hadron decays (see later), the ψ' yield is expected to be approximately 20 times smaller than the J/ψ yield. The number of ψ' obtained from the fit is compatible with the expected number. For completeness, the fit has been repeated for electron and muon pairs separately. In the electron case, the J/ψ signal is 356 events and the background 141 events. In the muon case, the signal and background are 385 and 95 events, respectively.

The efficiency of the J/ψ selection algorithm has been calculated using the MC sample containing 10 000 J/ψ mesons produced in b-quark decays. The following corrections and systematic uncertainties[3] have been considered (see Table 1):

[3] All percentage errors and corrections in this paper are relative to central values.

- The MC events have been generated using the Peterson fragmentation function for b-quarks. The average energy of the primary b-hadron, scaled by the beam energy, has been measured experimentally, in a model dependent way using the JETSET 7.3 version of the MC generator, to be $\langle x_E \rangle_{\rm b} = 0.713 \pm 0.012$ [29] (since the JETSET 7.4 version of the generator is used in this analysis, the result has been corrected by +0.016 to take into account the inclusion of resonances with orbital momentum L=1). The uncertainty in $\langle x_E \rangle_{\rm b}$ results in a 0.8% error in the efficiency.

- The MC momentum distribution of J/ψ in the rest frame of the decaying b-hadron has been reweighted to match the distribution measured by CLEO in Υ(4S) decays [9]. Taking into account both the statistical uncertainties in this distribution and the difference in b-hadron composition, the corresponding efficiency error is estimated to be 0.6%.

- The MC generator does not include radiative J/ψ decays into lepton pairs. These radiative decays produce a tail towards lower values in the invariant mass distribution, especially significant in the electron case. The result is a drop in efficiency of (12.4 ± 0.8)% for electrons and (3.7 ± 0.4)% for muons. The photon spectrum calculated in [30] using first order perturbative QED has been used to obtain this result. The uncertainties take into account an estimation of higher order QED corrections [31] and detector simulation effects.

- According to the MC, 2.6% of the J/ψ events have only one reconstructed lepton track inside the acceptance region ($p > 2$ GeV/c and $|\cos\theta| < 0.9$). A systematic error of 1.3%, equivalent to 50% of the number of events lost, has been assigned to account for the uncertainty in this effect.

- Efficiency of the lepton selection for $|\cos\theta| < 0.7$:
  The track selection requires for both electrons and muons a certain number of quality cuts, in particular a z chamber match and a minimum number of $\mathrm{d}E/\mathrm{d}x$ hits. The efficiency of this cut has been obtained by comparing data and MC events for inclusive muon pairs with invariant mass in the range 2.0-4.0 GeV/c^2, passing all J/ψ selection cuts except the track quality cuts. The result of this analysis is that the MC reproduces the efficiency of the track quality cuts with 3.1% accuracy; this number includes both statistical and MC background modelling uncertainties. The efficiency of the lepton selection in the central region of the detector, after applying the track quality cuts, has been studied as in [23]. The result of this analysis is an uncertainty of 2.0% in the MC modelling of these efficiencies, both in the electron and in the muon case. The efficiency uncertainties for lepton pairs are taken to be 4.0%, assuming totally correlated errors for the two tracks.

- Efficiency of the lepton selection for $|\cos\theta| > 0.7$:
  The efficiency of the lepton selection in the forward region of the detector, relative to the central part, is determined by comparing the angular distributions, obtained in data and MC, of all tracks in inclusive lepton pairs, with invariant mass between 2.0 and 4.0 GeV/c^2, passing all other selection criteria as J/ψ candidates. These distributions, normalised in the region $|\cos\theta| < 0.7$, are shown in Fig. 3. The MC reproduces accurately the lepton-pair efficiency in the forward region, relative to the central part. The corresponding uncertainty in the global J/ψ selection efficiency is 1.9%; this error includes both the statistical and the MC background modelling uncertainty.

- The effect of material around the beam pipe is important in determining the electron efficiency. The MC describes this material with better than 10% accuracy [23], resulting in an electron efficiency uncertainty of 3.8% .

- The J/ψ signal from $\mu^+\mu^-$ pairs can be described by a Gaussian with a mean of (3101$\pm$5) MeV/c^2 (compatible with the nominal J/ψ mass from the Particle Data Group (PDG) of 3097 MeV/c^2

[32]) and a width of (62 ± 4) MeV/c^2. The uncertainties in the mean and the width lead to a systematic error in the efficiency of 0.6% for electrons and 0.2% for muons.

error source	$\Delta\epsilon(ee)$	$\Delta\epsilon(\mu\mu)$	$\Delta\epsilon(\mathrm{J}/\psi)$
b-quark fragmentation	0.8 %	0.8 %	0.8 %
J/ψ momentum distribution	0.6 %	0.6 %	0.6 %
final state radiation	0.8 %	0.4 %	0.6 %
track reconstruction	1.3 %	1.3 %	1.3 %
track quality cuts	3.1 %	3.1 %	3.1 %
lepton eff.($\lvert\cos\theta\rvert < 0.7$)	4.0 %	4.0 %	2.8 %
lepton eff.($\lvert\cos\theta\rvert > 0.7$)	1.9 %	1.9 %	1.9 %
detector radiation losses	3.8 %	–	1.6 %
invariant mass resolution	0.6 %	0.2 %	0.4 %
MC statistics	2.9 %	2.8 %	2.0 %
total error	7.5 %	6.3 %	5.6 %

Table 1: *Systematic errors in the calculation of the efficiency.*

The efficiency of the J/ψ selection algorithm is found to be $\epsilon_{\mathrm{J}/\psi} = (21.0 \pm 1.2)\%$, where the error includes all systematic uncertainties. The correlation between the electron and the muon efficiency errors has been taken into account in obtaining the total error. According to the MC, the efficiency for muon pairs is 30% larger than for electron pairs, in agreement with the observed number of events in these two channels.

3.3 Inclusive branching ratios

The Z^0 branching ratio to J/ψ is calculated as follows:

$$Br(\mathrm{Z}^0 \to \mathrm{J}/\psi\ X) = \frac{N_{\mathrm{J}/\psi}}{N_{\mathrm{had}}} \cdot \frac{\epsilon_{\mathrm{had}}}{\epsilon_{\mathrm{J}/\psi}} \cdot \frac{R_{\mathrm{had}}}{2Br(\mathrm{J}/\psi \to \ell^+\ell^-)}$$

where $N_{\mathrm{J}/\psi}$ is the number of J/ψ candidates (corrected for background), N_{had} is the number of multihadronic events, ϵ_{had} and $\epsilon_{\mathrm{J}/\psi}$ are their respective selection efficiencies, $R_{\mathrm{had}} = \Gamma_{\mathrm{had}}/\Gamma_{\mathrm{Z}} = 0.699 \pm 0.002$ [32], and $Br(\mathrm{J}/\psi \to \ell^+\ell^-) = (5.91 \pm 0.23)\%$ [33] (where ℓ can be either an electron or a muon, which explains the factor 2 in front of the leptonic branching ratio in the above formula). This leptonic branching ratio has been used in all previous LEP measurements of the inclusive J/ψ ratio, except in the original OPAL result [5].

In order to calculate the selection efficiency, the origin of the J/ψ meson must be known. According to MC calculations, the efficiency to select J/ψ mesons produced in fragmentation processes via the 'colour-octet' mechanism is 5% smaller than for those produced in b-hadron decays, due to their softer momentum spectrum. According to [3], the J/ψ fragmentation yield in Z^0 decays is

$$Br(\mathrm{Z}^0 \to \mathrm{prompt\ J}/\psi) = (3.3^{+3.3}_{-1.6}) \cdot 10^{-4},$$

assuming a factor 2 uncertainty in this calculation. This theoretical prediction is compatible with the measurement presented by DELPHI in [8], although a direct comparison is not possible since this measurement was obtained assuming a 'colour-singlet' J/ψ production mechanism. In the following, the 'colour-octet' yield is used to obtain an effective selection efficiency. This effective efficiency is smaller than the efficiency from b-hadron decays alone by only $(0.4 \pm 0.3)\%$. Taking this into account, the inclusive decay ratio of Z^0 into J/ψ mesons is:

$$Br(\mathrm{Z}^0 \to \mathrm{J}/\psi\ X) = (3.9 \pm 0.2 \pm 0.3) \cdot 10^{-3},$$

where the first error is statistical and the second systematic (see Table 2 for a detailed list of errors).

error source	$\Delta Br(\mathrm{Z}^0 \to \mathrm{J}/\psi\ X)$	$\Delta Br(\mathrm{b} \to \mathrm{J}/\psi\ X)$
$\epsilon_{\mathrm{J}/\psi}$	5.6 %	5.6 %
N_{bkg}	3.5 %	3.5 %
ϵ_{had}	0.5 %	0.5 %
R_{had}	0.5 %	–
R_{b}	–	1.5 %
$Br(\mathrm{J}/\psi \to \ell^+\ell^-)$	3.9 %	3.9 %
fragm. component	0.3 %	6.2 %
systematic error	7.7 %	9.9 %
statistical error	5.3 %	5.3 %
total error	9.3 %	11.2 %

Table 2: *Summary of errors in the measurement of inclusive branching ratios.*

This result is compatible with the previous OPAL measurement [5], and in good agreement with other LEP measurements (see Table 3 which includes the previous OPAL measurement, scaled to account for the latest $Br(\mathrm{J}/\psi \to \ell^+\ell^-)$ measurement). It corresponds to an average J/ψ multiplicity in hadronic Z^0 decays of:

$$\langle N_{\mathrm{J}/\psi} \rangle = (5.6 \pm 0.3 \pm 0.4) \cdot 10^{-3}.$$

Measurement	Ref.	$Br(\mathrm{Z}^0 \to \mathrm{J}/\psi\ X)$
OPAL	[5]	$(5.3 \pm 0.9 \pm 0.5) \cdot 10^{-3}$
ALEPH	[6]	$(3.8 \pm 0.4 \pm 0.3) \cdot 10^{-3}$
L3	[7]	$(3.6 \pm 0.5 \pm 0.4) \cdot 10^{-3}$
DELPHI	[8]	$(3.7 \pm 0.4 \pm 0.4) \cdot 10^{-3}$
OPAL	this work	$(3.9 \pm 0.2 \pm 0.3) \cdot 10^{-3}$

Table 3: *LEP measurements of* J/ψ *production in* Z^0 *decays.*

The inclusive branching ratio of b-quarks to J/ψ mesons is calculated as follows:

$$Br(\mathrm{b} \to \mathrm{J}/\psi\ X) = \frac{N^{\mathrm{b}}_{\mathrm{J}/\psi}}{N_{\mathrm{had}}} \cdot \frac{\epsilon_{\mathrm{had}}}{\epsilon_{\mathrm{J}/\psi}} \cdot \frac{1}{2R_{\mathrm{b}} \cdot 2Br(\mathrm{J}/\psi \to \ell^+\ell^-)},$$

where $N^{\mathrm{b}}_{\mathrm{J}/\psi}$ is the number of J/ψ candidates produced in b-quark decays and $R_{\mathrm{b}} = \Gamma_{\mathrm{b\bar{b}}}/\Gamma_{\mathrm{had}} = 0.221 \pm 0.003$ [32] . As discussed before, a small fraction of J/ψ candidates originate from fragmentation processes. After subtracting this component from $N_{\mathrm{J}/\psi}$, based on the 'colour-octet' yield prediction quoted above, the result is:

$$Br(\mathrm{b} \to \mathrm{J}/\psi\ X) = (1.15 \pm 0.06 \pm 0.12)\%,$$

where the errors are again detailed in Table 2. It is noted that the fragmentation component is in this case an important contribution to the total systematic error. This result is in good agreement with the measurement performed in $\Upsilon(4\mathrm{S})$ decays [9], $Br(\mathrm{B}^{0,\pm} \to \mathrm{J}/\psi\ X) = (1.12 \pm 0.07)\%$. The difference in b-hadron composition is not expected to produce any substantial difference between the two measurements. Theoretical predictions for this branching ratio range between 0.2% and 2% (see discussion in [9] and references therein).

3.4 b-quark fragmentation

The momentum distribution of J/ψ candidates can be used to study the fragmentation function of b-quarks. Fig. 4 shows the normalised momentum distribution, after subtracting the background and correcting for efficiency (see also Table 4).

$x_p = p/E_{\rm beam}$	$(1/N) \cdot (\mathrm{d}N/\mathrm{d}x_p)$
$0.0 - 0.1$	–
$0.1 - 0.2$	0.097 ± 0.033
$0.2 - 0.3$	0.125 ± 0.021
$0.3 - 0.4$	0.194 ± 0.025
$0.4 - 0.5$	0.262 ± 0.025
$0.5 - 0.6$	0.212 ± 0.022
$0.6 - 0.7$	0.070 ± 0.012
$0.7 - 0.8$	0.030 ± 0.007
$0.8 - 0.9$	0.009 ± 0.004
$0.9 - 1.0$	0.001 ± 0.001

Table 4: *Normalised momentum distribution of* J/ψ *candidates, after subtracting the background and correcting for efficiency. The errors are bin-to-bin uncorrelated. There is in addition a bin-to-bin systematic correlated error of 7%, not included in the table.*

The momentum distribution of background events was obtained from $e^{\pm}\mu^{\mp}$ pairs, in the same way as the total background. The MC J/ψ momentum distribution based on the Peterson fragmentation function for b-quarks was fitted to the data, using $\langle x_E \rangle_{\rm b}$ as the only fit parameter. The optimum value for this parameter was found to be $\langle x_E \rangle_{\rm b} = 0.709 \pm 0.012$, where the error is only statistical. The χ^2 of this fit is 0.6 per degree of freedom. The following systematic error sources were considered: uncertainties in the background and efficiency determination, final state radiation and radiation in the detector material, the fragmentation component (shown in Fig. 4), the J/ψ momentum distribution in the rest frame of the decaying b-hadron (discussed previously), and finally the b-quark fragmentation model (the same models as in [29] were considered). The contribution of each individual source to the total systematic error is detailed in Table 5. The central value was obtained assuming that the fragmentation component is described by [3]. The final result is:

$$\langle x_E \rangle_{\rm b} = 0.709 \pm 0.012 \pm 0.013,$$

the first error being statistical and the second systematic. This result is in good agreement with the inclusive lepton result [29], $\langle x_E \rangle_{\rm b} = 0.713 \pm 0.006 \pm 0.011$, which has been corrected as explained previously. Since the J/ψ in b-hadron decays carries a larger fraction of the energy than inclusive leptons in b-hadron semileptonic decays, the J/ψ momentum spectrum provides an increased sensitivity to the b-quark fragmentation function, relative to the inclusive lepton spectrum, but suffers from considerably reduced statistics. This inclusive measurement of $\langle x_E \rangle_{\rm b}$ is also in agreement with measurements based on samples of B^0 and B^+ decaying into D-mesons and leptons [34].

4 Inclusive ψ' production

4.1 ψ' reconstruction

Once a J/ψ candidate is identified, ψ' mesons can be reconstructed using the decay $\psi' \to \mathrm{J}/\psi\ \pi^+\pi^-$, which has a branching ratio $Br(\psi' \to \mathrm{J}/\psi\ \pi^+\pi^-) = (32.4 \pm 2.6)\%$ [32].

error source	$\Delta\langle x_E\rangle_{\rm b}$
background	0.004
efficiency	0.004
radiative decays	0.001
detector radiation	0.002
fragm. component	0.004
momentum at rest	0.005
fragmentation model	0.008
MC statistics	0.005
total error	0.013

Table 5: *Systematic errors in the measurement of* $\langle x_E\rangle_{\rm b}$.

A different J/ψ selection, optimised to maximise efficiency rather than minimise systematic errors, was used in this part of the analysis. Leptons were selected inside the larger acceptance region $|\cos\theta| < 0.95$. Electrons were identified by a neural net algorithm as in [35] and photon conversions were rejected as in the inclusive J/ψ analysis. Muons were identified using the same algorithm as in the inclusive J/ψ analysis or by an algorithm including the hadron calorimeter outside the acceptance of the muon chambers, as in [29]. Otherwise the J/ψ selection proceeded as before. The efficiency of the above J/ψ selection is, according to the MC, $(32.1 \pm 0.4)\%$ for the inclusive J/ψ sample, corrected for final state radiation as discussed previously, the error being only statistical. The number of J/ψ candidates found in this way is, after background subtraction,

$$N_{\rm J/\psi} = 718 \pm 32 \pm 25,$$

where the first error is statistical and the second results from the background subtraction; the uncertainty on the background subtraction under the J/ψ peak has been estimated as in the inclusive analysis.

In addition to the MC samples used in the inclusive analysis, a sample of 6000 MC events containing the decay chain $\rm Z^0 \to b(\overline{b}) \to \psi' \to J/\psi\ \pi^+\pi^-$, and the subsequent decay $\rm J/\psi \to \ell^+\ell^-$, has been generated to optimize selection criteria and to compute efficiencies. In these events the $\pi^+\pi^-$ invariant mass distribution has been generated according to the measured one [33]. ψ' mesons have been reconstructed by associating to each J/ψ candidate a pair of tracks fulfilling the following requirements:

- The two tracks must have opposite charge.
- The angle between each track and the J/ψ direction must be smaller than 90°.
- The momentum of each track must exceed 400 MeV/c.
- The invariant mass of the two charged tracks must be, under the pion hypothesis, in the range 0.45-0.60 GeV/c^2. This range is optimized to reject the background[4].
- The impact parameter of each track with respect to the J/ψ vertex must be compatible with the hypothesis of a common vertex, within 3 standard deviations.

The mass of the ψ' is calculated after kinematically constraining the lepton pair mass to the nominal J/ψ mass. The invariant mass distribution obtained in this way is displayed in Fig. 5. In order to calculate the background, the invariant mass distribution has been fitted using a binned

[4]The observed $\pi^+\pi^-$ invariant mass distribution is consistent with the hypothesis of a quasiparticle in this mass range.

maximum likelihood method. The fitting function consists of a Gaussian to describe the signal and a second order polynomial to describe the background. The ψ' signal can be described by a Gaussian with a mean of (3688 ± 2) MeV/c^2 and a width of (7 ± 2) MeV/c^2. The mean value agrees with the nominal ψ' mass of 3686 MeV/c^2 [32]. ψ' candidates were selected by demanding an invariant mass in the range 3662–3712 MeV/c^2, corresponding to 2.5 standard deviations in the MC around the nominal ψ' mass. The number of ψ' candidates, obtained by subtracting the calculated background from the observed number of candidates in the signal region, is:

$$N_{\psi'} = 46.9 \pm 9.7 \pm 3.9,$$

where the first error is statistical and the second results from the background subtraction.

4.2 Inclusive branching ratio

The efficiency to select a J/ψ is the same for a J/ψ produced directly in a b-hadron decay and for a J/ψ produced in a cascade decay through a ψ', within the uncertainties discussed below. The ratio of inclusive branching ratios from Z^0 decays is therefore:

$$\frac{Br(Z^0 \to \psi'\ X)}{Br(Z^0 \to J/\psi\ X)} = \frac{N_{\psi'}}{N_{J/\psi}} \cdot \frac{1}{\epsilon_{\psi'}} \cdot \frac{1}{Br(\psi' \to J/\psi\ \pi^+\pi^-)},$$

where $\epsilon_{\psi'}$ is defined as the efficiency to find a $\psi' \to J/\psi\ \pi^+\pi^-$ decay once a J/ψ has been selected. According to the MC, $\epsilon_{\psi'} = (49.5 \pm 1.6)\%$, where the error is only statistical.

The following systematic uncertainties on the ratio of branching ratios have been considered (see summary in Table 6):

- The uncertainties on the J/ψ and ψ' backgrounds have been determined as described above.
- Most systematic uncertainties connected to the J/ψ selection efficiency cancel out in the ratio, and can be neglected. The J/ψ detection efficiency depends however on the J/ψ momentum and thus on its production mechanism. This uncertainty on the production mechanism has been studied using MC calculations and the momentum spectra in the rest frame of the decaying b-hadron, measured by CLEO [9].
- The MC resolutions for track parameters in r-ϕ (track curvature κ, distance of closest approach to the coordinate origin d_0, and azimuthal angle at the point of closest approach ϕ_0) and in z (tangent of the dip angle $\tan\lambda$ and the z-coordinate at the point of closest approach z_0) were tuned to describe the data. These track parameter resolutions were further varied by 10% in r-ϕ and 30% in z to obtain the corresponding systematic error in the efficiency.

Error source	Error
J/ψ background	3.5 %
ψ' background	8.2 %
J/ψ eff. ratio	1.5 %
ψ' efficiency	5.5 %
$Br(\psi' \to J/\psi\ \pi^+\pi^-)$	8.0 %
MC statistics	3.2 %
total error	13.6 %

Table 6: *Summary of systematic uncertainties on the ratio of branching ratios.*

Including all uncertainties, the result is:

$$\frac{Br(\mathrm{Z}^0 \to \psi'\, X)}{Br(\mathrm{Z}^0 \to \mathrm{J}/\psi\, X)} = 0.41 \pm 0.09 \pm 0.06,$$

where the first error is statistical and the second systematic. The branching ratio $Br(\mathrm{Z}^0 \to \psi'\, X)$ can be obtained using the result of the inclusive J/ψ analysis:

$$Br(\mathrm{Z}^0 \to \psi'\, X) = (1.6 \pm 0.3 \pm 0.2) \cdot 10^{-3},$$

in agreement with a previous DELPHI measurement [8] of $Br(\mathrm{Z}^0 \to \psi'\, X) = (1.6 \pm 0.7 \pm 0.3) \cdot 10^{-3}$, and corresponds to an average ψ' multiplicity in hadronic Z^0 decays of:

$$\langle N_{\psi'} \rangle = (2.3 \pm 0.4 \pm 0.3) \cdot 10^{-3}.$$

The corresponding b-quark decay ratio can be extracted, after subtracting the expected contribution from ψ' produced in fragmentation processes. According to [3], the prompt ψ' yield in Z^0 decays is:

$$Br(\mathrm{Z}^0 \to \text{prompt } \psi') = (1.0^{+1.0}_{-0.5}) \cdot 10^{-4},$$

assuming again a factor 2 uncertainty in this calculation. Taking this into account, the following result is obtained:

$$Br(\mathrm{b} \to \psi'\, X) = (0.49 \pm 0.10 \pm 0.09)\%,$$

in agreement with the result obtained in Υ(4S) decays [9], $Br(\mathrm{B}^{0,\pm} \to \psi'\, X) = (0.34 \pm 0.05)\%$.

5 Exclusive b-hadron reconstruction using J/ψ decays

5.1 b-hadron reconstruction

Candidate b-hadrons can be reconstructed by combining the J/ψ with other particles in the event. In this analysis, the low-multiplicity modes[5] $\mathrm{B}^0 \to \mathrm{J}/\psi\, \mathrm{K}^0_\mathrm{S}$, $\mathrm{B}^0 \to \mathrm{J}/\psi\, \mathrm{K}^{*0}$, $\mathrm{B}^+ \to \mathrm{J}/\psi\, \mathrm{K}^+$, $\mathrm{B_s} \to \mathrm{J}/\psi\, \phi$ and $\Lambda_\mathrm{b} \to \mathrm{J}/\psi\, \Lambda$, where all the decay products can be identified without excessive combinatorial backgrounds, were considered. J/ψ candidates were selected as in the ψ' analysis. In addition to the MC samples used in the inclusive analysis, samples of 1250 exclusive J/ψ events in each of the various decay modes were generated and used to calculate the corresponding selection efficiencies.

The following requirements were applied in all modes:

- All added tracks were required to lie in the same thrust hemisphere as the J/ψ.
- All added tracks, except those from K^0_S or Λ decays, were required to have an impact parameter with respect to the J/ψ vertex, d_0 (with error Δd_0), satisfying $|d_0| < 0.03$ cm, and $|d_0|/\Delta d_0 < 2$.
- Charged kaons were required to satisfy $w^K_{\mathrm{d}E/\mathrm{d}x} > 5\%$ if their $\mathrm{d}E/\mathrm{d}x$ was above the expected value for kaons at their measured momentum ($w_{\mathrm{d}E/\mathrm{d}x}$ is the probability of measuring the observed specific ionisation $\mathrm{d}E/\mathrm{d}x$). This requirement provides good kaon identification against the majority pionic background. Charged kaon momenta were required to exceed 2 GeV/c. This requirement reduces the low-momentum combinatorial background and puts the kaon above the region where the $\mathrm{d}E/\mathrm{d}x$ versus momentum curves for kaons and pions cross.
- The number of hits used for the calculation of $\mathrm{d}E/\mathrm{d}x$ was required to be at least 10 for all charged kaons and pions, except those from K^0_S or Λ decays.

[5] Charge conjugation is implied throughout.

- The momentum of the reconstructed b-hadron was required to exceed 25 GeV/c. This provides good rejection of combinatorial background owing to the hardness of b fragmentation.

The following requirements were applied to individual modes:

- $B^0 \to J/\psi\, K^0_S$: the K^0_S were identified via their $\pi^+\pi^-$ decay mode. They were identified using a procedure based on a search for a displaced V^0 vertex. The selection is the same as in [36] without d_0 cuts, in order to increase the efficiency. A cut of $0.467 \leq m_{K^0_S} \leq 0.527$ GeV/c^2 was applied on the mass of the reconstructed K^0_S.

- $B^0 \to J/\psi K^{*0}$: the K^{*0} were identified via their $K^+\pi^-$ decay mode. A cut of $0.836 \leq m_{K^{*0}} \leq 0.956$ GeV/c^2 was applied on the mass of the reconstructed K^{*0}. The momentum of the π^- was required to exceed 1 GeV/c, and its $w^{\pi}_{dE/dx}$ was required to exceed 2.5% if its dE/dx was below the expected value for a pion, and 0.1% if it was above.

- $B^+ \to J/\psi\, K^+$: no additional cuts were applied.

- $B_s \to J/\psi\, \phi$: the ϕ were identified via their K^+K^- decay mode. A cut of $0.999 \leq m_\phi \leq 1.039$ GeV/c^2 was applied on the mass of the reconstructed ϕ. To reduce backgrounds from reflections of $B^0 \to J/\psi\, K^{*0}$ decays where the pion is misidentified as a kaon, the mass of the pair of kaon candidates under the kaon-pion hypothesis was required to be below 0.850 GeV/c^2.

- $\Lambda_b \to J/\psi\, \Lambda$: the Λ were identified via their $p\pi^-$ decay mode, using a similar algorithm as for the K^0_S. A cut of $1.100 \leq m_\Lambda \leq 1.130$ GeV/c^2 was applied on the mass of the reconstructed Λ. The momentum of the Λ was required to exceed 4 GeV/c.

Kinematic fitting, using the SQUAW package [37], was employed to improve mass resolutions. In this way, the mass resolution in the mode $B_s \to J/\psi\, \phi$, for example, was improved from 100 MeV/c^2 to 45 MeV/c^2, according to the MC. In these fits, the J/ψ, K^0_S, ϕ and Λ were kinematically constrained to their nominal masses, but not the K^{*0}, since this particle is a wide resonance for which kinematic fitting is problematic. The χ^2 probability for the overall kinematic fit, including all particles involved in the b-hadron decay, was required to exceed 1%. The invariant mass distributions are shown in Fig. 6, where several modes are added in both data and MC, and in Fig. 7, where all individual modes are displayed. B^+ and B^0 candidates were selected in the mass range 5.15–5.40 GeV/c^2, B_s candidates in the range 5.30–5.45 GeV/c^2, and finally Λ_b candidates in the range 5.50–5.80 GeV/c^2. These mass ranges correspond approximately to two standard deviations, according to MC, around the nominal particle masses [32]. The number of candidates found in each mode, $N_{\rm cand}$, is listed in Table 7.

5.2 Branching ratio determination

The efficiencies of the above selections (excluding the efficiency of the J/ψ selection and the branching ratios of K^0_S, K^{*0}, ϕ and Λ decays), estimated from the exclusive MC samples, are shown in Table 7, where the errors are statistical only.

Both the combinatorial background and that originating from physics processes is obtained for the first three modes in a MC-independent way by performing an unbinned extended maximum likelihood fit [38] to the mass distribution, as illustrated in Fig. 6 for the sum of the three modes. The probability density function consists of a Gaussian whose width is the event-by-event candidate mass error for the signal, and an exponential for the background. The fit parameters are the position of the Gaussian (corresponding to the fitted b-hadron mass), the slope of the exponential and the fraction of the background component (corresponding to the fraction of background in the mass distribution). This simple parametrisation was chosen after consideration of the possible backgrounds. The random combinatorial background is not expected to produce any structure beyond the usual exponential fall-off. Physics background can come either from reflections, where one particle is misidentified as another,

Mode	efficiency(%)	$N_{\rm cand}$	$N_{\rm B}$
$\rm B^0 \to J/\psi\, K^0_S$	34.0 ± 2.5	10	$8.4 \pm 3.2 \pm 0.1$
$\rm B^0 \to J/\psi\, K^{*0}$	23.0 ± 1.9	4	$3.1^{+2.6}_{-1.6} \pm 0.1$
$\rm B^+ \to J/\psi\, K^+$	47.5 ± 2.3	12	$9.2 \pm 3.5 \pm 0.1$
$\rm B_s \to J/\psi\, \phi$	22.8 ± 1.9	2	$1.9^{+2.0}_{-1.0} \pm 0.1$
$\Lambda_{\rm b} \to \rm J/\psi\, \Lambda$	21.7 ± 2.2	–	–

Table 7: *Reconstruction efficiencies, number of candidates, $N_{\rm cand}$, and number of background subtracted candidates, $N_{\rm B}$, for each decay mode. The errors on the efficiencies are statistical only. The first error on the number of b-hadrons is statistical and the second results from the background subtraction.*

or from satellites, where one or more particles are missed. The former can lead to a significant peak in the signal region, and the cuts were chosen to reduce such backgrounds. The latter will typically produce structure located below the signal region. In the absence of any visible structure in either data or MC (see again Fig. 6) this is taken to be subsumed in the exponential. The exponential resulting from the fits (see Fig. 7) is used to calculate the expected background inside the invariant mass windows defined for each decay mode. The number of background subtracted candidates, $N_{\rm B}$, is obtained in each individual mode by subtracting this background from the total number of candidates $N_{\rm cand}$ (see Table 7). In the $\rm B_s \to J/\psi\, \phi$ mode, the background is directly estimated from the MC. No signal is observed in the $\Lambda_{\rm b} \to \rm J/\psi\, \Lambda$ channel; in all the other modes the probability of the expected background fluctuating to the observed number of events in the signal region or more is below 10%.

The product branching ratios are then determined. For example, the product branching ratio for the mode $\rm B_s \to J/\psi\, \phi$ is calculated as:

$$f(\bar{b} \to \rm B_s) \cdot Br(B_s \to J/\psi\, \phi) = \frac{N_{\rm B}}{N_{\rm had}} \cdot \frac{\epsilon_{\rm had}}{2R_{\rm b} \cdot 2Br(J/\psi \to \ell^+\, \ell^-) \cdot Br(\phi \to K^+\, K^-) \cdot \epsilon_{J/\psi} \cdot \epsilon_\phi}$$

where $f(\bar{b} \to \rm B_s)$ is the production rate of $\rm B_s$ by b-quarks from $\rm Z^0$ decays, $\epsilon_{J/\psi}$ is the selection efficiency for the $\rm J/\psi$ in this particular b-hadron decay mode, ϵ_ϕ is the selection efficiency for the ϕ assuming a $\rm J/\psi$ has been identified, and all other quantities have already been defined. It is noted that the $\epsilon_{J/\psi}$ values are typically 10% larger than the inclusive efficiency, since they involve only two body decays of b-hadrons. The product branching ratios can further be converted into branching ratios by dividing by the production rates for each b-hadron from b-quarks, which are taken to be $(39.5 \pm 3.0)\%$ for each of $\rm B^+$ and $\rm B^0$, $(12.0 \pm 4.0)\%$ for $\rm B_s$, and $(8.0 \pm 4.0)\%$ for $\Lambda_{\rm b}$, as in [39].

The following systematic errors were considered (see Table 8):

- In order to obtain the error on the efficiencies, the modelling of track parameters was varied as in the inclusive ψ' analysis.
- $\rm d\mathit{E}/d\mathit{x}$ particle identification. The MC models the $\rm d\mathit{E}/d\mathit{x}$ distributions with uncertainties of about 1% on the mean and 15% on the width. These values are conservative in view of the results obtained in [40]. These values were used to evaluate the corresponding systematic errors in the efficiencies.
- For b-quark fragmentation, the same procedure as in the inclusive analysis was applied.
- The uncertainty on the $\rm J/\psi$ selection efficiency was estimated by comparing the inclusive $\rm J/\psi$ branching ratio obtained with the present lepton selection and the inclusive branching ratio measured in the inclusive analysis.

- The errors on the branching ratios for J/ψ, K^0_S, K^{*0}, ϕ and Λ decays were taken from [32]. For R_b, the error previously quoted was used.
- For b-hadron production rates, the errors quoted above were used.
- The MC statistical errors include, in addition to the uncertainty in the efficiencies reported in Table 7, a component due to the J/ψ selection efficiency in each decay mode, and a component from the uncertainty on ϵ_{had}.

error source	$B^0 \to J/\psi\, K^0_S$	$B^0 \to J/\psi\, K^{*0}$	$B^+ \to J/\psi\, K^+$	$B_s \to J/\psi\, \phi$	$\Lambda_b \to J/\psi\, \Lambda$
track parameters	14 %	12 %	6 %	12 %	14 %
particle dE/dx	–	7 %	1 %	5 %	–
b fragmentation	2 %	5 %	3 %	3 %	10 %
J/ψ selection eff.	8 %	8 %	8 %	8 %	8 %
branching ratios	4 %	4 %	4 %	4 %	4 %
production rates	8 %	8 %	8 %	33 %	50 %
MC statistics	8 %	9 %	6 %	9 %	11 %
total error	20 %	21 %	15 %	38 %	55 %

Table 8: *Systematic errors in the determination of branching ratios for each decay mode.*

The branching ratios obtained, together with their statistical and systematic errors, are listed in Table 9. The value for the $\Lambda_b \to J/\psi\,\Lambda$ mode corresponds to a product branching ratio 90% C.L. upper limit of $f(b \to \Lambda_b) \cdot Br(\Lambda_b \to J/\psi\,\Lambda) < 2.4 \cdot 10^{-4}$.

Mode	$Br/10^{-3}$	PDG	$m_B(\mathrm{GeV}/c^2)$	PDG
$B^0 \to J/\psi\, K^0_S$	$1.22 \pm 0.46 \pm 0.24$	0.38 ± 0.11	$5.269 \pm 0.009 \pm 0.004$	5.279 ± 0.002
$B^0 \to J/\psi\, K^{*0}$	< 1.9 @ 90% C.L.	1.58 ± 0.28	$5.288 \pm 0.023 \pm 0.007$	5.279 ± 0.002
$B^+ \to J/\psi\, K^+$	$0.78 \pm 0.30 \pm 0.12$	1.02 ± 0.14	$5.298 \pm 0.012 \pm 0.003$	5.279 ± 0.002
$B_s \to J/\psi\, \phi$	< 7.4 @ 90% C.L.	'seen'	$5.367 \pm 0.015 \pm 0.005$	5.375 ± 0.006
$\Lambda_b \to J/\psi\, \Lambda$	< 4.2 @ 90% C.L.	'seen'	–	5.641 ± 0.050

Table 9: *Branching ratios and reconstructed b-hadron masses obtained for each decay mode, with statistical and systematic errors. The PDG values are given for comparison.*

5.3 Mass determination

The fitting procedure also returns, as discussed above, the invariant masses of B^0 and B^+ mesons. The B_s mass is calculated from a weighted average of the two candidate events. The following systematics were considered (see Table 10):

- Modelling of track parameters. This effect was studied as above, by varying the resolution of track parameters, and taking the shift in fitted mass as the systematic error.
- Uncertainty in the absolute mass scale. Studies of the K^0_S mass have shown that reconstructed track momenta could be shifted by at most 0.25%. This effect was consequently studied by shifting all momenta on input to the kinematic fitter by 0.25%, again taking the shift in fitted mass as the systematic error.

error source	$B^0 \to J/\psi\, K^0_S$	$B^0 \to J/\psi\, K^{*0}$	$B^+ \to J/\psi\, K^+$	$B_s \to J/\psi\, \phi$
track parameters	4 MeV/c^2	2 MeV/c^2	2 MeV/c^2	1 MeV/c^2
mass scale	1 MeV/c^2	7 MeV/c^2	2 MeV/c^2	5 MeV/c^2
total error	4 MeV/c^2	7 MeV/c^2	3 MeV/c^2	5 MeV/c^2

Table 10: *Systematic errors in the determination of masses for each decay mode.*

The invariant masses obtained, together with their statistical and systematic errors, are shown in Table 9, and are consistent with the PDG values. The B_s mass obtained in this analysis is consistent with a previous OPAL result [13] based on the observation of only one of the two B_s candidates.

5.4 Search for B_c

B_c mesons have not yet been observed. A summary of the expected properties of these particles, according to theoretical calculations, is given below (see a review in [41] and references therein). The mass is expected to be 6.25 GeV/c^2, with a spread between the various models smaller than 0.05 GeV/c^2, and the lifetime in the range 0.4–0.9 ps. They can be produced in b-quark and c-quark fragmentation processes, but the second mechanism is expected to provide a negligible contribution to the total yield, as shown in [41]. The probability that a b-quark hadronises into a B_c, either directly or via the decay of excited states, is expected to be $f(\bar{b} \to B_c) \approx 9 \cdot 10^{-4}$, but this prediction has a factor 2 uncertainty. Since the B_c contains a constituent c-quark, the inclusive branching ratio of B_c into J/ψ is expected to be much larger than for other b-hadrons, around 20%, but exclusive branching ratios are likely to be small. For example the mode $B_c \to J/\psi\, \pi^+$ is expected to have a branching ratio between 0.2% and 0.4%.

A search for B_c was performed in the decay mode $B_c \to J/\psi\, \pi^+$. The selection of J/ψ candidates and general requirements for this particular mode were the same as for the other exclusive modes, namely:

- The pion track was required to lie in the same thrust hemisphere as the J/ψ.
- The pion track was required to have an impact parameter with respect to the J/ψ vertex, satisfying $|d_0| < 0.03$ cm and $|d_0|/\Delta d_0 < 2$.
- The number of hits used for the calculation of the charged pion $\mathrm{d}E/\mathrm{d}x$ was required to be at least 10.
- The momentum of the reconstructed B_c was required to exceed 25 GeV/c.

The following requirements were applied to this particular mode:

- The momentum of the pion was required to exceed 4 GeV/c.
- $w^{\pi}_{\mathrm{d}E/\mathrm{d}x}$ was required to exceed 2.5% if $\mathrm{d}E/\mathrm{d}x$ was below the expected value for a pion, and 0.1% if it was above.

Kinematic fitting was employed as before to improve the B_c mass resolution. The invariant mass distribution is shown in Fig. 7. B_c candidates were selected in the mass range 6.0–6.5 GeV/c^2, corresponding to approximately 2 standard deviations around the expected B_c mass. The invariant mass uncertainty includes both the experimental resolution and the theoretical uncertainty. Only 1 candidate was found in this mass interval, with a mass of $6.31 \pm 0.17 \pm 0.01$ GeV/c^2, the first error resulting from the kinematical fit and the second from the uncertainty in the mass scale, calculated

as for the other modes. The expected background was calculated using the inclusive J/ψ MC sample and resulted to be (0.3 ± 0.1) events. The observed event is compatible with the expected background.

A sample of 1250 multihadronic events including a B_c and the subsequent decays $B_c \to J/\psi\,\pi^+$ and $J/\psi \to \ell^+\ell^-$, was generated using the JETSET 7.4 MC as before, in order to determine the selection efficiency. For the momentum distribution of the primary B_c, two distributions were considered: the distribution provided by JETSET 7.4 and the distribution proposed in [41], approximated by a Peterson function with $\epsilon_b = m_c^2/(2m_b)^2 \approx 0.021$. The efficiency was obtained by averaging the efficiencies obtained with these two models. The efficiency for the J/ψ selection was found to be $(31.1 \pm 1.2)\%$ and the efficiency to detect the pion, once the J/ψ is reconstructed, was found to be $(33.7 \pm 2.2)\%$, the errors being only statistical. The following systematic errors were considered in the calculation of the product branching ratio $f(\bar{b} \to B_c) \cdot Br(B_c \to J/\psi\,\pi^+)$ (see Table 11): the modelling of track parameters and dE/dx, the b-quark fragmentation, the uncertainty on the J/ψ selection efficiency, the errors on the branching ratio for J/ψ decays and on R_b, and finally the MC statistical error. All these errors, except the fragmentation error, were calculated as for the other b-hadron decay modes. For the fragmentation error, a larger variation of the $\langle x_E \rangle_b$ parameter has been considered to account for uncertainties in the fragmentation mechanism. The difference between the two models used for the fragmentation of the B_c resulted in a $\pm 13\%$ variation in the efficiency. The theoretical uncertainties in the B_c mass and lifetime resulted in negligible contributions to the total uncertainty.

error source	$B_c \to J/\psi\,\pi^+$
track parameters	5 %
pion dE/dx	5 %
b fragmentation	13 %
J/ψ selection eff.	8 %
branching ratios	4 %
MC statistics	9 %
total error	19 %

Table 11: *Summary of systematic errors used in the determination of the upper limit to the product branching ratio* $f(\bar{b} \to B_c) \cdot Br(B_c \to J/\psi\,\pi^+)$.

Taking into account the observed candidate and the systematic error, the following 90% C.L. upper limit is obtained for B_c production in b-quark decays:

$$f(\bar{b} \to B_c) \cdot Br(B_c \to J/\psi\,\pi^+) < 2.1 \cdot 10^{-4}.$$

6 Summary

The fraction of events containing a J/ψ meson in Z^0 decays has been measured using a sample of 3.6 million hadronic events collected by OPAL between 1990 and 1994. The result of this analysis is:

$$Br(Z^0 \to J/\psi\ X) = (3.9 \pm 0.2 \pm 0.3) \cdot 10^{-3},$$

where the first error is statistical and the second systematic. The b-quark decay ratio into J/ψ is measured to be:

$$Br(b \to J/\psi\ X) = (1.15 \pm 0.06 \pm 0.12)\%,$$

assuming that J/ψ candidates originate predominantly in b-quark decays. The momentum distribution of J/ψ candidates is used to study the fragmentation function of b-quarks. The average scaled energy of the primary b-hadron produced in the fragmentation process is found to be:

$$\langle x_E \rangle_b = 0.709 \pm 0.012 \pm 0.013,$$

assuming the Peterson model for b-quark fragmentation, implemented in the framework of the JETSET 7.4 MC generator.

The inclusive J/ψ sample is used to reconstruct ψ' mesons decaying into a J/ψ and a $\pi^+\pi^-$ pair. The corresponding inclusive decay ratio is measured to be:

$$Br(\mathrm{Z}^0 \to \psi'\ X) = (1.6 \pm 0.3 \pm 0.2) \cdot 10^{-3}.$$

The b-quark decay ratio into ψ' is measured to be:

$$Br(\mathrm{b} \to \psi'\ X) = (0.49 \pm 0.10 \pm 0.09)\%,$$

assuming that ψ' candidates originate predominantly in b-quark decays.

Finally, the inclusive J/ψ sample is used to reconstruct b-hadron candidates by combining the J/ψ with other particles in the event. The low-multiplicity modes $\mathrm{B}^0 \to \mathrm{J}/\psi \mathrm{K}^0_\mathrm{S}$, $\mathrm{B}^0 \to \mathrm{J}/\psi \mathrm{K}^{*0}$, $\mathrm{B}^+ \to \mathrm{J}/\psi \mathrm{K}^+$, $\mathrm{B_s} \to \mathrm{J}/\psi\,\phi$ and $\Lambda_\mathrm{b} \to \mathrm{J}/\psi\,\Lambda$, are considered. After background subtraction, the number of candidates for the first four modes is found to be 8.4, 3.1, 9.1 and 1.9, respectively, and no candidate is found in the last mode. These fully reconstructed candidates are used to calculate b-hadron decay ratios and masses, as given in Table 9. A search for $\mathrm{B_c}$ mesons is performed in the mode $\mathrm{B_c} \to \mathrm{J}/\psi\,\pi^+$, yielding the following 90% C.L. upper limit for $\mathrm{B_c}$ production in b-quark decays:

$$f(\bar{b} \to \mathrm{B_c}) \cdot Br(\mathrm{B_c} \to \mathrm{J}/\psi\,\pi^+) < 2.1 \cdot 10^{-4}.$$

Acknowledgements

It is a pleasure to thank the SL Division for the efficient operation of the LEP accelerator, the precise information on the absolute energy, and their continuing close cooperation with our experimental group. In addition to the support staff at our own institutions we are pleased to acknowledge the
Department of Energy, USA,
National Science Foundation, USA,
Particle Physics and Astronomy Research Council, UK,
Natural Sciences and Engineering Research Council, Canada,
Fussefeld Foundation,
Israel Ministry of Science,
Israel Science Foundation, administered by the Israel Academy of Science and Humanities,
Minerva Gesellschaft,
Japanese Ministry of Education, Science and Culture (the Monbusho) and a grant under the Monbusho International Science Research Program,
German Israeli Bi-national Science Foundation (GIF),
Direction des Sciences de la Matière du Commissariat à l'Energie Atomique, France,
Bundesministerium für Forschung und Technologie, Germany,
National Research Council of Canada,
Hungarian Foundation for Scientific Research, OTKA T-016660.

References

[1] The various 'colour-singlet' models are the following:
The 'charm fragmentation' process, $Z^0 \to c\bar{c}$ followed by $c(\bar{c}) \to J/\psi c(\bar{c})$:
E.Braaten, K.Cheung and T.C.Yuan, Phys.Rev. **D48** (1993) 4230,
V.Barger, K.Cheung and W.Y.Keung, Phys.Rev. **D41** (1990) 1541.
The 'gluon fragmentation' process, $Z^0 \to q\bar{q}g$ followed by $g \to J/\psi$ gg:
E.Braaten and T.C.Yuan, Phys.Rev.Lett. **71** (1993) 1673,
K.Hagiwara, A.D.Martin and W.J.Stirling, Phys.Lett. **B267** (1991) 527,
erratum **B316** (1993) 631.
The 'gluon radiation' process, $Z^0 \to J/\psi gg$:
W.Y.Keung, Phys.Rev. **D23** (1981) 2072,
J.H.Kühn and H.Schneider, Z.Phys. **C11** (1981) 263.
The first process is dominant according to theoretical calculations.

[2] M.Cacciari et al., *Charmonium Production at the Tevatron*,
CERN-TH/95-129.

[3] P.Cho, *Prompt Upsilon and Psi Production at LEP*, CALT-68-2020,
K.Cheung, W.Y. Keung and T.C.Yuan, *Colour-Octet Quarkonium Production at the Z Pole*,
FERMILAB-PUB-95/300-T.

[4] J.H.Kühn, S.Nussinov and R.Rückl, Z.Phys. **C5** (1980) 117.

[5] OPAL Collab., G.Alexander et al., Phys.Lett. **B266** (1991) 485.

[6] ALEPH Collab., D.Buskulic et al., Phys.Lett. **B295** (1992) 396.

[7] L3 Collab., O.Adriani et al., Phys.Lett. **B317** (1993) 467.

[8] DELPHI Collab., P.Abreu et al., Phys.Lett. **B341** (1994) 109.

[9] CLEO Collab., R.Balest et al., Phys.Rev. **D52** (1995) 2661.

[10] H.Fritzsch, Phys.Lett. **B86** (1979) 164,
H.Fritzsch, Phys.Lett. **B86** (1979) 343.

[11] CDF Collab., F.Abe et al., Phys.Rev.Lett. **72** (1994) 3456.

[12] CLEO Collab., M.S.Alam et al., Phys.Rev. **D50** (1994) 43.

[13] OPAL Collab., P.D.Acton et al., Phys.Lett. **B295** (1992) 357,
OPAL Collab., R.Akers et al., Phys.Lett. **B337** (1994) 196.

[14] ALEPH Collab., D.Buskulic et al., Phys.Lett. **B311** (1993) 425.

[15] CDF Collab., F.Abe et al., Phys.Rev.Lett. **71** (1993) 1685.

[16] DELPHI Collab., P.Abreu et al., Phys.Lett. **B324** (1994) 500.

[17] UA1 Collab., C.Albajar et al., Phys.Lett. **B273** (1991) 540.

[18] CDF Collab., F.Abe et al., Phys.Rev. **D47** (1993) 2639.

[19] OPAL Collab., K.Ahmet et al., Nucl. Instrum. and Meth. **A305** (1991) 275.

[20] OPAL Collab., P.Allport et al., Nucl. Instrum. and Meth. **A324** (1993) 34,
OPAL Collab., P.Allport et al., Nucl. Instrum. and Meth. **A346** (1994) 476.

[21] M.Hauschild et al., Nucl. Instrum. and Meth. **A314** (1992) 74.

[22] OPAL Collab., G.Alexander et al., Z.Phys. **C52** (1991) 175.

[23] OPAL Collab., P.D.Acton et al., Z.Phys. **C58** (1993) 523.

[24] T.Sjöstrand, Computer Physics Commun. **82** (1994) 74,
T.Sjöstrand, JETSET 7.4 Manual, CERN-TH.7112/93.

[25] OPAL Collab., G.Alexander et al., *A Comparison of b and uds quark jets to gluon jets,* CERN-PPE/95-126, submitted to Z.Phys.

[26] J.Allison et al., Nucl.Instrum. and Meth. **A317** (1992) 47.

[27] C.Peterson et al., Phys.Rev. **D27** (1983) 105.

[28] OPAL Collab., P.D.Acton et al., Z.Phys. **C60** (1993) 19.

[29] OPAL Collab., R.Akers et al., Z.Phys. **C60** (1993) 199.

[30] F.A.Berends and R.Kleiss, Nucl.Phys. **B177** (1981) 237.

[31] O.Nicrosini and L.Trentadue, Phys.Lett. **B196** (1987) 551,
J.P.Alexander et al., Phys.Rev. **D37** (1988) 56.

[32] L.Montanet et al., Review of Particle Properties, Phys.Rev. **D50** (1994) 1173.

[33] MARK-III Collab., D.Coffman et al., Phys.Rev.Lett. **68** (1992) 282.

[34] OPAL Collab., G.Alexander et al., *A study of b Quark Fragmentation into* B^0 *and* B^+ *Mesons at LEP,* CERN-PPE/95-122, submitted to Phys.Lett B.

[35] OPAL Collab., R.Akers et al., Phys.Lett. **B327** (1994) 411.

[36] OPAL Collab., P.D.Acton et al., Phys.Lett. **B298** (1993) 456.

[37] O.Dahl et al., The SQUAW package, LBL Group A, Programming note P-126(1968).

[38] R.Barlow, Nucl. Instrum. and Meth. **A297** (1990) 496.

[39] OPAL Collab., R.Akers et al., Z.Phys. **C66** (1995) 555.

[40] OPAL Collab., R.Akers et al., Z.Phys. **C63** (1994) 181.

[41] A.Leike and R.Rückl, *Production of heavy bound states at LEP and beyond*, MPI-PhT/94-41.

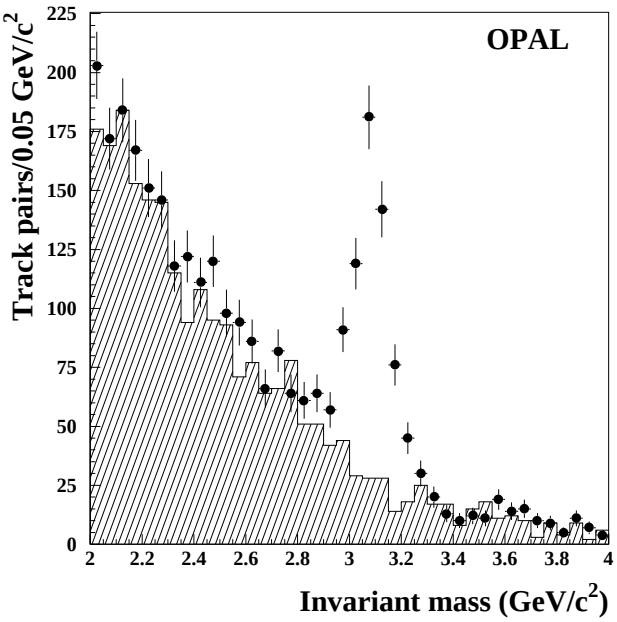

Figure 1: Invariant mass of e^+e^- and $\mu^+\mu^-$ pairs. The shaded histogram of $e^\pm\mu^\mp$ pairs used to calculate the background is superimposed.

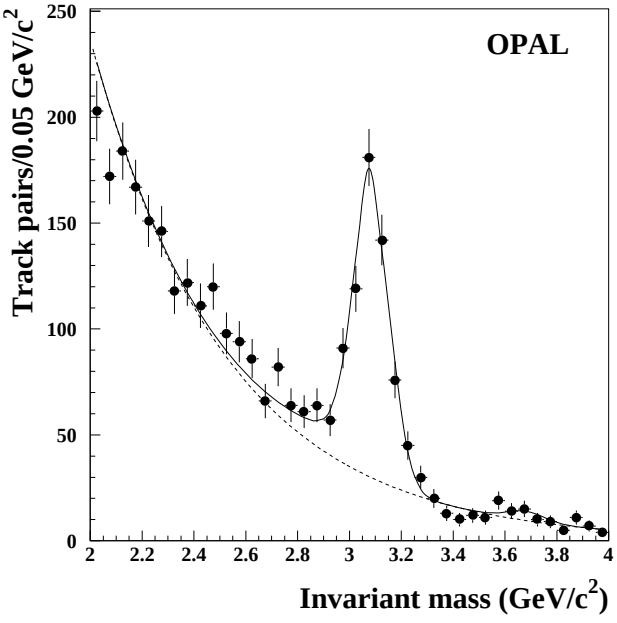

Figure 2: Invariant mass of e^+e^- and $\mu^+\mu^-$ pairs. The background exponential function and the two Gaussians with radiative tails used in the fit are shown. The two Gaussians describe the J/ψ and ψ' signals.

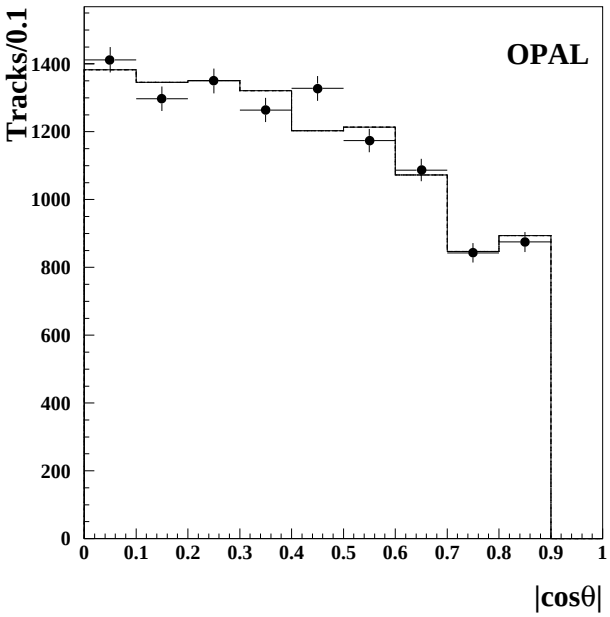

Figure 3: Angular distribution of all tracks in selected lepton pairs with invariant mass between 2.0 and 4.0 GeV/c^2. The points are data and the histogram MC. The distributions are normalised for $|\cos\theta| < 0.7$.

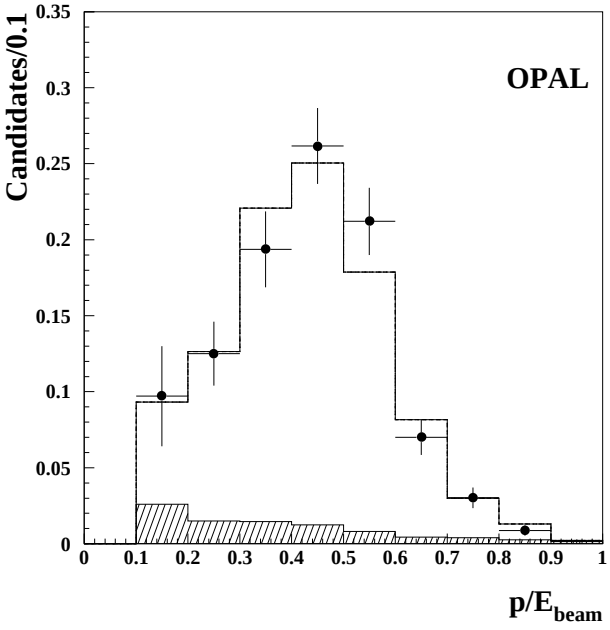

Figure 4: Normalised momentum distribution of J/ψ candidates, after subtracting the background and correcting for efficiency. The points correspond to data, the histogram to a MC distribution using the Peterson fragmentation model, and the hatched distribution to the fragmentation component.

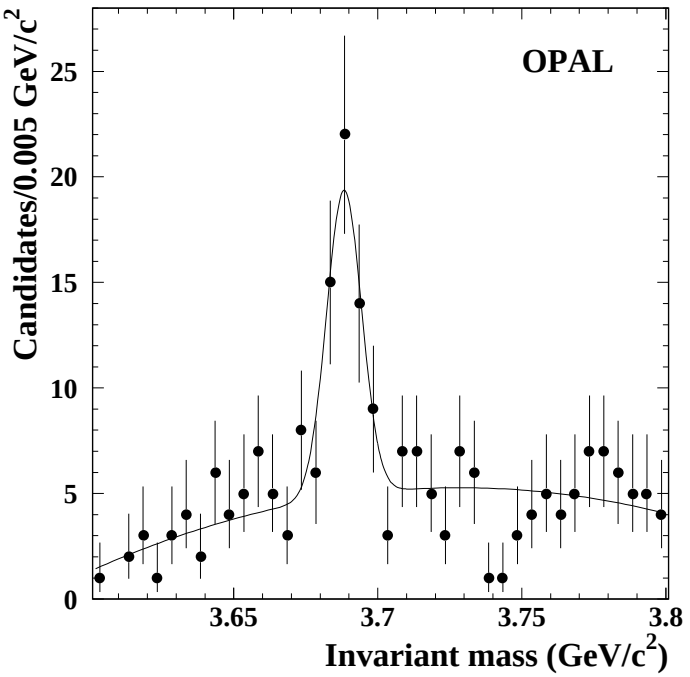

Figure 5: Invariant mass distribution of ψ' candidates. The data are fitted with a Gaussian to describe the signal and a second order polynomial to describe the background.

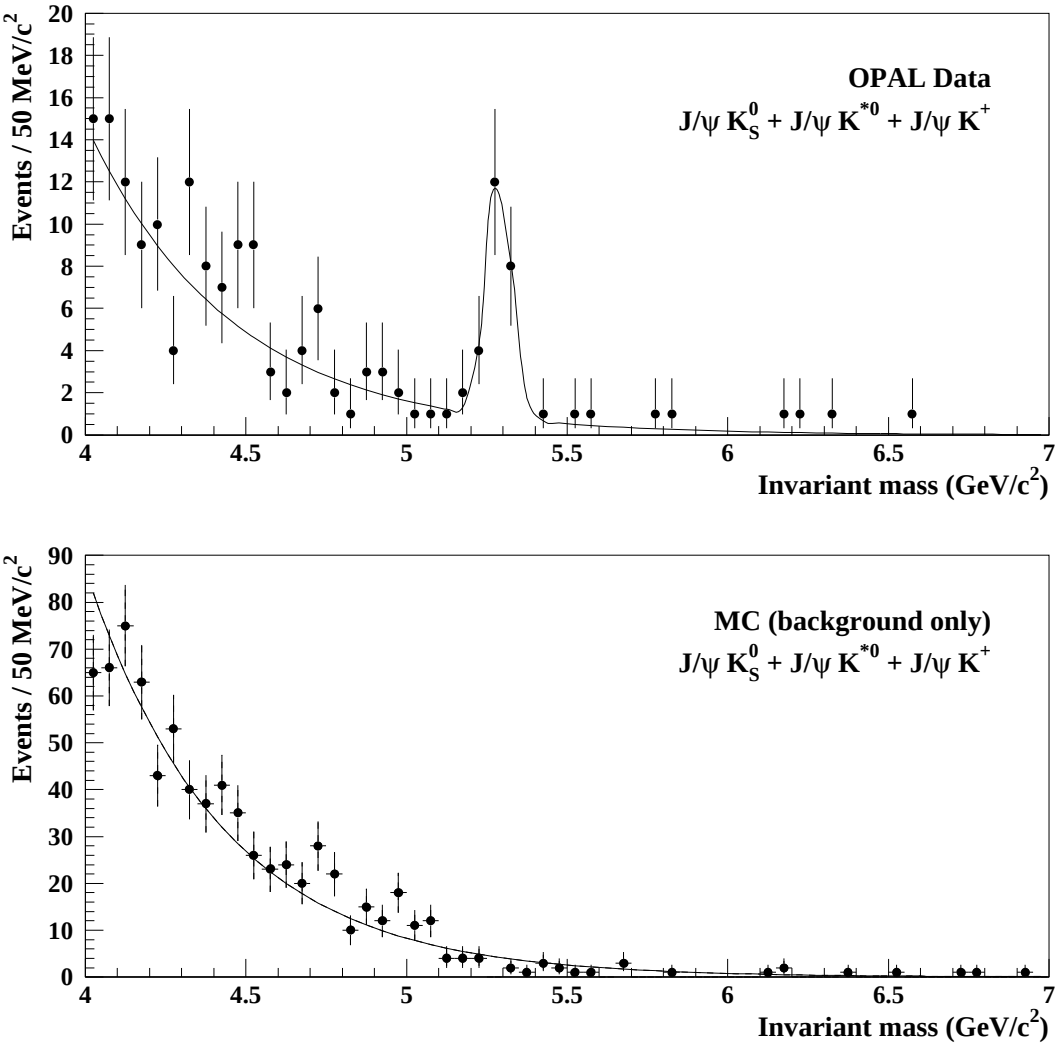

Figure 6: Mass spectra of the three modes $B^+ \to J/\psi K^+$, $B^0 \to J/\psi K^0_S$ and $B^0 \to J/\psi K^{*0}$ for data and MC (where only the background is shown). Fits using an exponential for the background are overlaid.

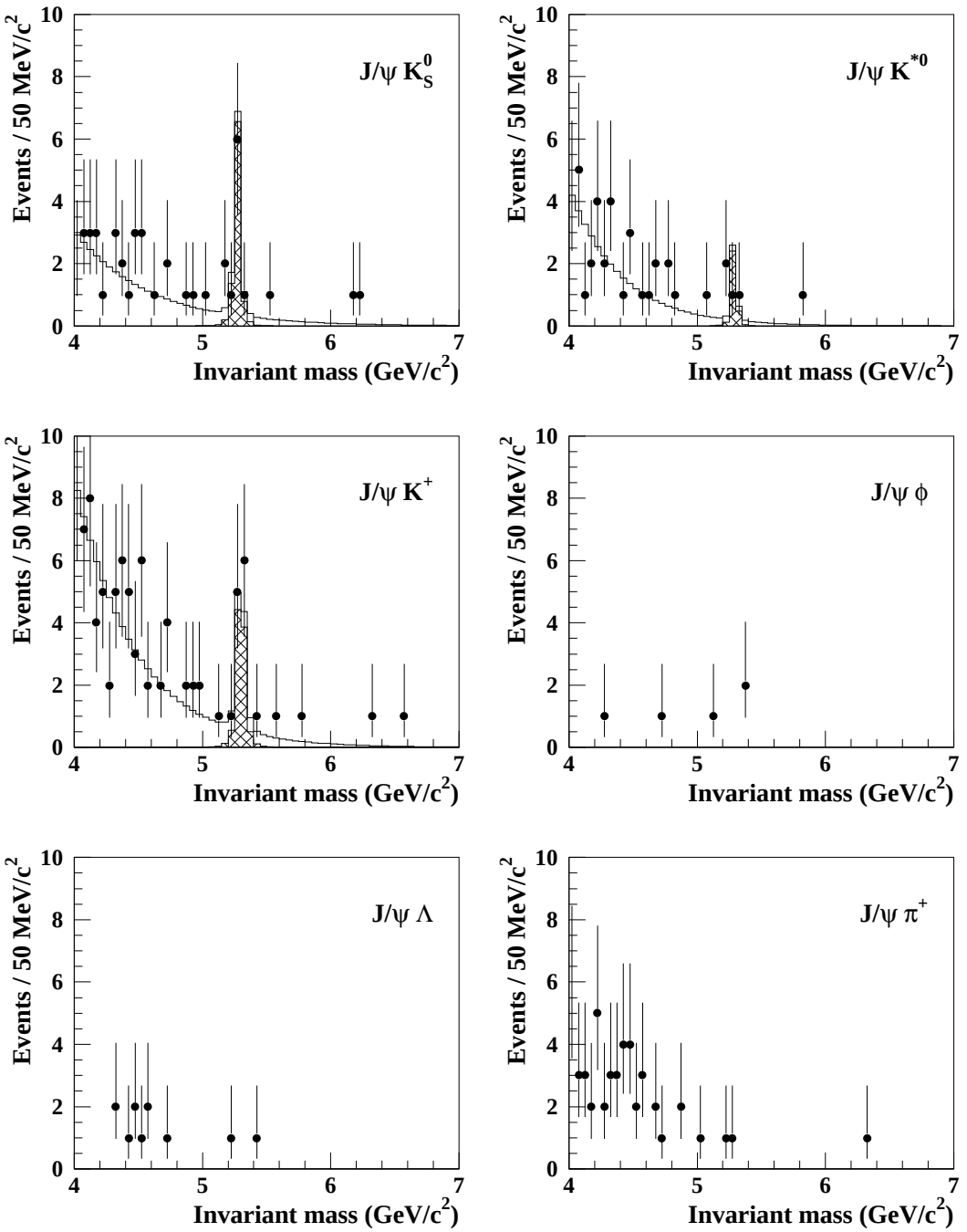

Figure 7: The mass spectra for the modes $B^0 \to J/\psi\, K^0_S$, $B^0 \to J/\psi\, K^{*0}$, $B^+ \to J/\psi\, K^+$, $B_s \to J/\psi\, \phi$, $\Lambda_b \to J/\psi\, \Lambda$ and $B_c \to J/\psi\, \pi^+$, respectively. The points are the data, the solid line the maximum likelihood fitted probability distribution function (p.d.f.), and the hashed area the fitted p.d.f. for the signal.